

1993

Three-dimensional imaging of living neurons and glia with the atomic force microscope

Vladimir Parpura
Iowa State University

Philip G. Haydon
Iowa State University

Eric Henderson
Iowa State University, telomere@iastate.edu

Follow this and additional works at: http://lib.dr.iastate.edu/zool_pubs

 Part of the [Cell Biology Commons](#), [Developmental Biology Commons](#), and the [Zoology Commons](#)

Recommended Citation

Parpura, Vladimir; Haydon, Philip G.; and Henderson, Eric, "Three-dimensional imaging of living neurons and glia with the atomic force microscope" (1993). *Zoology and Genetics Publications*. 22.
http://lib.dr.iastate.edu/zool_pubs/22

This Article is brought to you for free and open access by the Zoology and Genetics at Iowa State University Digital Repository. It has been accepted for inclusion in Zoology and Genetics Publications by an authorized administrator of Iowa State University Digital Repository. For more information, please contact digirep@iastate.edu.

Three-dimensional imaging of living neurons and glia with the atomic force microscope

Vladimir Parpura*, Philip G. Haydon and Eric Henderson

Signal Transduction Training Group, Department of Zoology and Genetics, Iowa State University, Ames, IA 50011, USA

*Author for correspondence

SUMMARY

The atomic force microscope (AFM) was used to directly image hippocampal neurons and glia. Using chemically fixed and living cells it was possible to reconstruct three-dimensional cell structure and detect sub-cellular features such as the nucleus, mitochondria and filaments. By repeatedly scanning a single living cell we observed the movement of filaments beneath the cell membrane. Furthermore, by controlling the force applied to the

scanning tip, nanosurgery was performed to selectively remove cells from the culture substratum. Thus, the atomic force microscope offers the opportunity to gain three-dimensional information about living cells and to observe the behavior of cellular components by imaging through the intact cell membrane.

Key words: AFM, living cells, nanosurgery

INTRODUCTION

During development of the nervous system the neuronal growth cone explores its local microenvironment, receiving signals from adjacent neurons and glia. Cell-cell signalling during these interactions is critical for the normal development of the brain. One approach to studying the growth cone is to image this dynamic structure in the light microscope and examine two-dimensional changes in morphology during cellular interactions. Higher-resolution, static images obtained by scanning electron microscopy are used to supplement light microscope information. It would be advantageous to be able to span the size range from molecules to entire cells in one microscope while imaging living specimens. The atomic force microscope (AFM) (Binnig et al., 1986), invented less than 10 years ago, has the potential to achieve this goal.

In the AFM a fine tip on the end of a small cantilever is scanned over the surface of interest. Deflections of the cantilever are recorded and displayed as a topographical map of the surface (Hansma et al., 1988). The AFM can image samples at extremely high, and in some cases atomic, resolution and has a sufficient dynamic range to allow imaging of structures such as lipids and proteins (Hansma et al., 1991), nucleic acids (Bustamante et al., 1992; Hansma et al., 1992; Henderson, 1992; Lindsay et al., 1989), membranes (Weisenhorn et al., 1991), gap junctions (Hoh et al., 1991), cells (Tomie et al., 1991) or groups of cells (Gould et al., 1990). It has been used to visualize the X-ray resist relief of living sperm (Tomie et al., 1991). In principle it should be possible to image cellular interactions and then

zoom into a defined location on the same cell to image molecular interactions. In this study we have used the AFM to image interactions between neurons and glia, observe dynamic surface and sub-membrane structures in these living cells, and perform nanosurgery on selected cells.

MATERIALS AND METHODS

Cells

Postnatal hippocampi were freshly dissected from 1- to 5-day-old Sprague-Dawley rat pups. Tissue was incubated for 1 hour at 36.8°C in Ca²⁺- and Mg²⁺-free Earle's balanced salt solution (EBSS, pH 7.35; Gibco) containing papain (20 i.u./ml; Sigma), Hepes (10 mM), L-cysteine (0.2 mg/ml), glucose (20 mM), penicillin (100 i.u./ml), streptomycin (100 µg/ml). Tissue was washed once with fresh EBSS and then placed in EBSS (pH 7.35) containing Hepes (10 mM) and trypsin inhibitor (10 mg/ml, type II-O; Sigma) for 5 minutes. After being rinsed, the hippocampi were mechanically dispersed by triturating through a fire-polished glass pipette. Cells were plated onto poly-L-lysine (1 mg/ml, *M_r* 10,000; Sigma)-coated glass coverslips (Fisher Scientific no. 1, 12 mm diameter) inlayed in a 35 mm culture dish. Cultures were maintained at 36.8°C in a humidified 5% CO₂/95% air atmosphere. Culture medium consisted of Eagle's minimum essential medium (Earle's salts; Gibco) supplemented 10% with heat-inactivated fetal bovine serum (Sigma) and containing 40 mM glucose, 2 mM L-glutamine, 1 mM pyruvate, 14 mM NaHCO₃, penicillin (100 i.u./ml) and streptomycin (100 µg/ml) (pH 7.35). All experiments were performed on cells that had been in culture for 1-4 days. The dissociation procedure was modified from previously described procedures (Heuttner and Baughman, 1986; Leifer et al., 1984; Mattson and Kater, 1989).

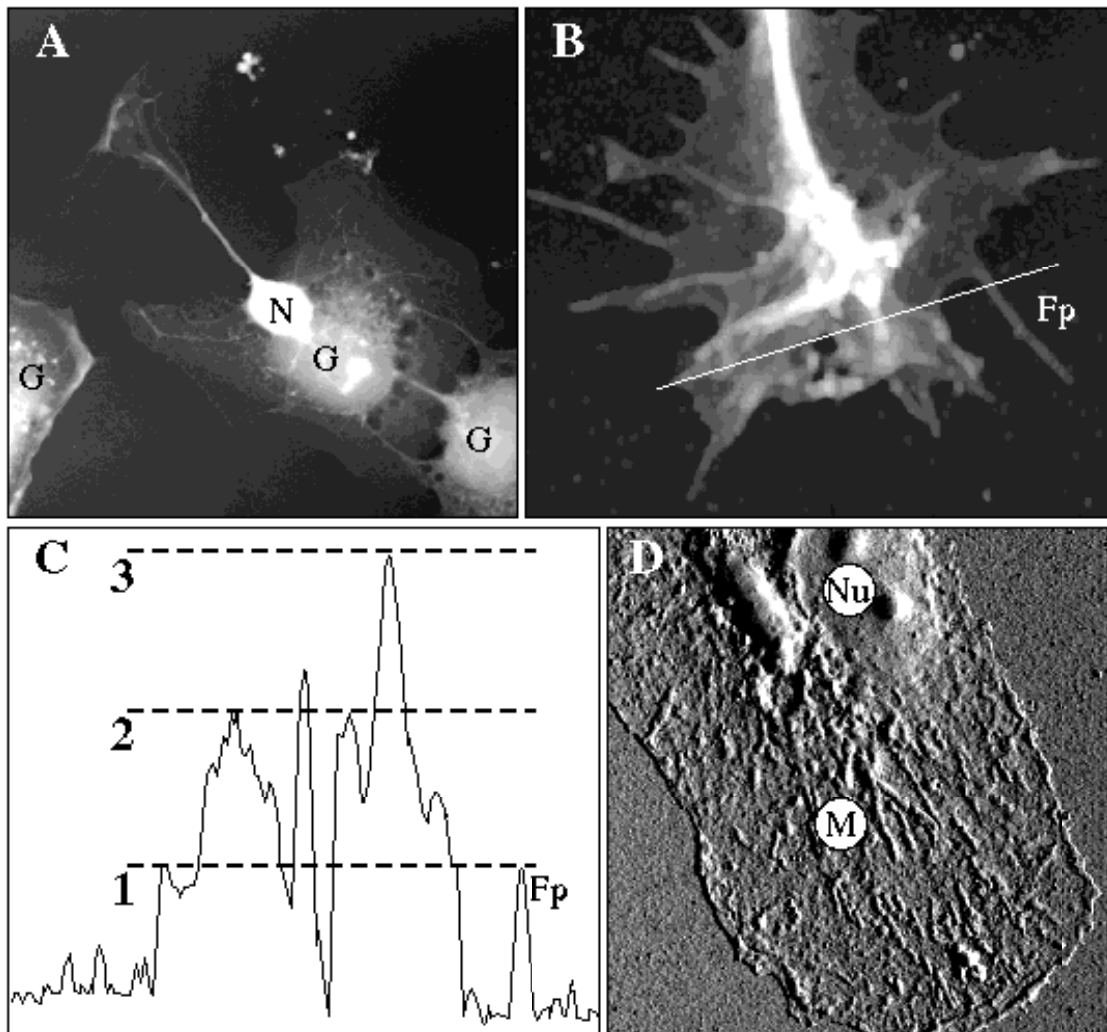


Fig. 1. Imaging of glutaraldehyde-fixed cells by the AFM. (A) A low-magnification image of a typical view of a hippocampal culture. In (B) a higher-magnification image of a typical hippocampal growth cone is shown. A section through this growth cone (C; white line in B) shows the height of the growth cone and a filopodium (Fp). The height of the filopodia of this growth cone is shown by the broken line labelled 1. The height of $2 \times$ and $3 \times$ the filopodial height is shown by the broken lines. Note that the growth cone has step changes in height which correspond in size to a multiple of the filopodial unitary height. In (D) a glial cell is shown and sub-cellular structures, such as the nucleus (Nu) and mitochondria (M) can be seen. Images shown in A and B were acquired in height mode while the image in D was acquired in error signal mode. The image sizes in A, B and D, were $70 \mu\text{m} \times 70 \mu\text{m}$, $18 \mu\text{m} \times 16 \mu\text{m}$ and $40 \mu\text{m} \times 40 \mu\text{m}$, respectively.

Fixation of cells

Cells were fixed for 30 minutes with 2.5% glutaraldehyde in EBSS containing 10.6 mM sodium citrate. After extensive washing, cells were dehydrated by addition of increasing concentrations of ethanol (50%, 70% and 95% each for 5 minutes) and were air dried.

Immunocytochemistry

Glia and neurons were identified in hippocampal cultures using antibodies directed against glial fibrillary acidic protein (GFAP; 1:1000, Sigma) and neuron-specific enolase (NSE; 1:4000, Polysciences), respectively. Antibody visualization was accomplished by using an Elite Kit (Vector) and the nickel-enhanced DAB method. Labelling was performed using techniques previously described by Lartius and Uemura (1990).

Mitochondrial staining

The size and distribution of mitochondria in living cells were determined by staining with a $10 \mu\text{M}$ solution of 4-(4-diethylaminostyryl)-*N*-methylpyridinium iodide (4-di₂ASP; Molecular Probes, Inc., Eugene, OR) (Lichtman et al., 1987).

AFM imaging

A Nanoscope III and associated equipment (Digital Instruments, Inc., Santa Barbara, CA) and Si_3N_4 gold-coated cantilevers with integral tips ("Nanoprobes", Digital Instruments, Inc., Santa Barbara, CA) were used in this study. To reveal height information (height mode imaging) the voltage controlling the movement of the piezo crystal is monitored. The accuracy of height information is limited to 0.1 nm. In error signal mode (ESM), the change in voltage from the photodetector due to cantilever movement is displayed directly. At high feedback gains, ESM accentuates changes in height rather than absolute height. When using living

cells we have found that ESM provides higher-contrast images of sub-cellular structures, although accurate height information is not resolved. All images were obtained at room temperature (22–24°C). Cantilevers had a reported spring constant of 0.12 N/m. All images of living cells were carried out in a fluid cell which maintained hydration and osmotic properties of the biological sample. Prior to imaging, cells were washed with imaging solution containing (in mM): NaCl, 150; CaCl₂, 2; Hepes, 10; KCl, 5; and MgCl₂, 2; pH 7.35; osmolarity, 330 mosM. Glass coverslips were mounted on metal discs and cells were imaged in a fluid cell using imaging solution filtered through a 0.22 μm filter. Imaging was carried out using a J scanner (132 μm × 132 μm) calibrated by the manufacturer (Digital Instruments, Inc., Santa Barbara, CA). The force during imaging and manipulations was monitored twice, prior to and immediately after images were captured, and calculated within 30 s. To prevent damage of the sample, the tip was engaged in a 0.1 μm × 0.1 μm area in the center of the sample and the force was initially adjusted to about 5 nN (nano Newton). The scan area was then enlarged and the images were collected immediately upon locating a feature of interest.

RESULTS AND DISCUSSION

To evaluate the potential of the AFM to image neural cells we first examined chemically fixed specimens. Mixed cultures of neurons and glia from rat hippocampi were fixed with glutaraldehyde, dehydrated and imaged in air. Fig. 1A shows a typical example of a scan containing a neuron (N) and glial cells (G). In this figure the neuron is attached to the surface of a glial cell. The processes and growth cone of the neuron can be traced on the glial cell and the structure of the glial cell can also be visualized. A higher-magnification image of a fixed neuronal growth cone, taken from a different cell, is shown in Fig. 1B. The height of

filopodia within an individual growth cone is constant. In the growth cone shown in Fig. 1B, the filopodial height is 64 ± 8 nm (mean \pm s.d.; $n = 14$). In seven other growth cones studied, a constant filopodial height was also detected within a given growth cone. However, the filopodial height ranged from 50 to 220 nm between different growth cones. From three-dimensional examinations of 8 growth cones, we observed step changes in growth cone height. The size of many of these steps is an integer multiple of the height of the attached filopodia (Fig. 1C). For example, step changes in growth cone height from about 60 to 120 to 180 nm are readily observed in this growth cone whose filopodia were about 60 nm thick. In other growth cones with a different filopodial height, step changes in growth cone height were also seen. However, the repeating step size was similar to the height of the attached filopodia. This suggests that filopodia of different growth cones may have different properties. Since filopodia are composed of actin filaments (Bridgman and Dailey, 1989) which extend from the body of the growth cone, it is possible that the repeating elements seen in growth cones are overlying actin bundles that arise from different filopodia.

In addition to imaging the surface topography of a cell, we have found that sub-cellular organelles can be revealed by scanning over the plasma membrane. Fig. 1D shows a glial cell imaged in error signal mode. Sub-cellular structures such as the cell nucleus (Nu) and mitochondria (M) are revealed in surprising detail. The size and distribution of mitochondria in living cells determined by staining with 4-di₂ASP correspond to the size and distribution of mitochondria imaged by AFM.

Using living cells we have been able to reliably obtain images of dynamic surface and sub-cellular events. Many of the structures detected by the AFM in fixed material were

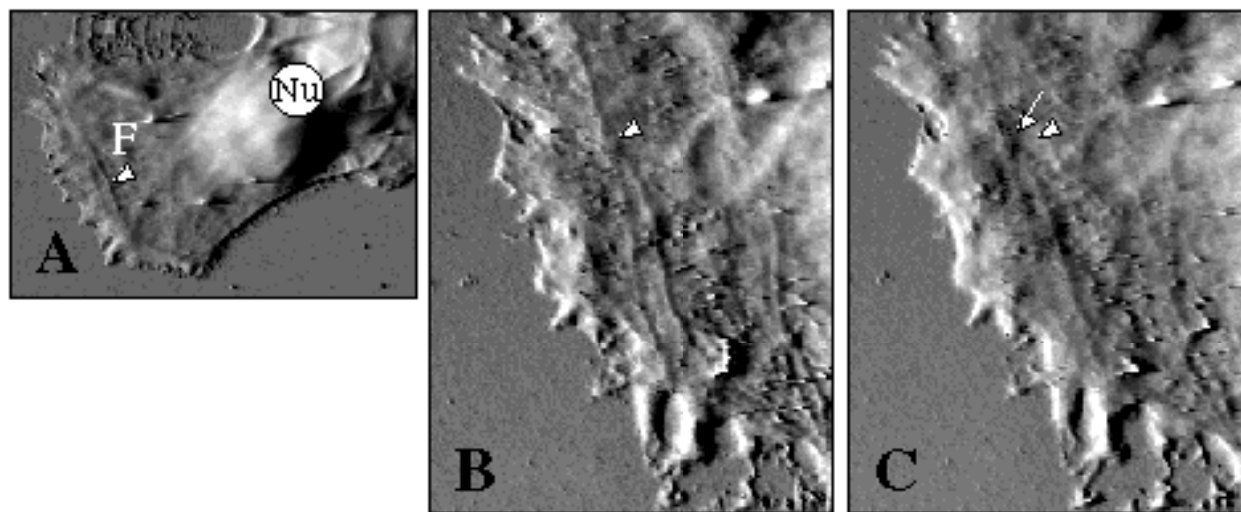


Fig. 2. Imaging of dynamic events in a living cell. In (A) an image of a living glial cell is shown. The nucleus (Nu) and filamentous (F; arrowhead) structures of this glial cell can be seen. In (B) and (C) higher-resolution images of the leading edge of this cell at two time points reveal the movement of a forked filamentous structure. In (B) and (C) the original position of the filament is marked with an arrowhead. Four minutes later in C the filament has moved 1.5 μm toward the stationary leading edge and its new position is marked with an arrow. Images were acquired in error signal mode with a force of 16 nN and image sizes were 60 μm × 75 μm in A and 35 μm × 28 μm in B and C.

also observed in living cells. Fig. 2A shows a living glial cell. The nucleus (Nu) as well as filamentous structures (F) can be seen. However, for unknown reasons, mitochondria have never been resolved in living cells. Imaging this glial cell at higher resolution reveals morphological changes over time in the leading edge as well as in the location of fila-

ments. Studies using the XR1 glial cell line from *Xenopus* (Henderson et al., 1992) have demonstrated that similar filaments are actin based. To best reveal these filaments and sub-cellular structures we found that a critical force had to be applied to the cell. In this preparation, as the force was increased from 5 to 16 nN the presence of filaments became

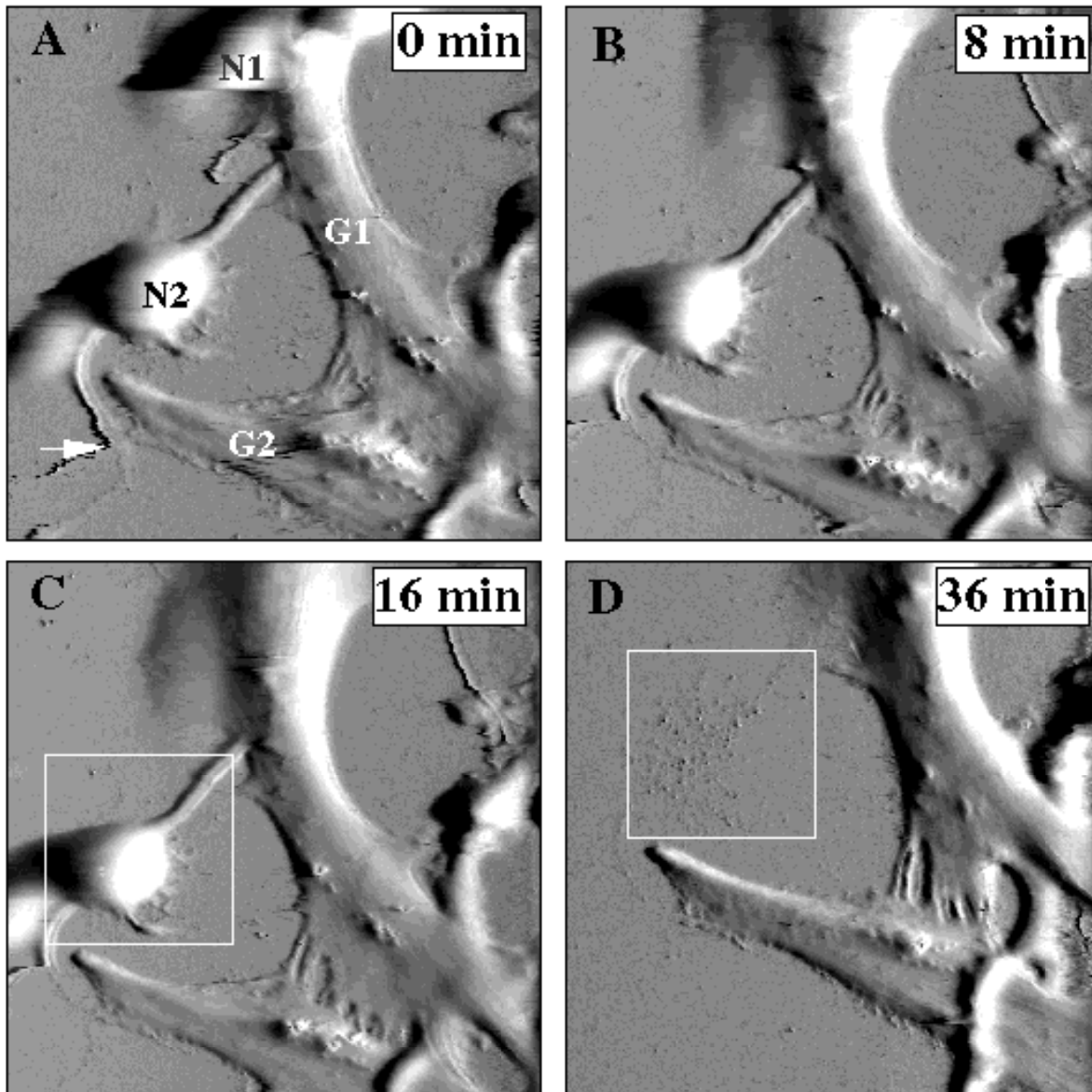


Fig. 3. Manipulation of living cells. The sequence of images A-D shows a temporal series that reveals morphological changes in living glial cells and demonstrates that the scanning tip can be used to selectively remove cells from the culture substratum. In (A) a force of 5 nN was used to image two neurons and two glial cells. With this force we are typically unable to detect filaments within glial cells. These filaments only become apparent when imaging forces are increased (see Fig. 2). During image acquisition neuron N1 was damaged by the scanning tip. Moreover, during the scan shown in A a neurite of the bipolar neuron N2 was cut by the scanning tip (arrow). In (B) the scanning force was increased to 10 nN and neuron N1 was completely removed from the field. Between C and D the area boxed in C was scanned with a force of 60 nN (image not shown) in an attempt to remove the neuron from the culture substratum. The success of this perturbation was confirmed by a subsequent full-field image (D; acquired with a force of 5 nN), which showed that the neuron had been removed from the substratum. Changes in glial cell shape and position were observed over time. Glial cell G1 became wider and thicker during the course of image acquisition. The width change is especially apparent when A and D are compared. Parameters used to capture images were: scan rate, 2 Hz; image size, $75 \mu\text{m} \times 75 \mu\text{m}$, and all images shown were acquired in error signal mode. Calculated heights were obtained from associated height mode images (not shown). Forces of 5 nN in A, C and D and 10 nN in B were used for image acquisition.

more pronounced. However, when excessive force was applied, the tip irreversibly injured the cell. The location of a forked filament is marked with an arrowhead at 0 minutes in Fig. 2B. Four minutes later (Fig. 2C) this filament had translocated by about 1.5 μm toward a stationary portion of the leading edge while other structures remained stationary. Thus, the AFM can reveal dynamic processes within living cells.

The ability to detect changes in cellular structures is further exemplified in Fig. 3, which shows a mixture of living neurons and glia. The width and thickness of a glial cell (G1) changed with time in culture. At its minimum width this glial cell measured 10 μm (Fig. 3A). However, 36 minutes later (Fig. 3D) the minimum width changed to 16 μm . Accompanying this change in cell width, the cell thickness changed from 0.7 to 1.2 μm at 20 and 32 minutes, respectively (data not shown). In addition to changes in cellular morphology, the shape of the cell-cell contacts between two glial cells (G1 and G2) changed over the course of the 36-minute imaging period.

A potential problem with the AFM is that the imaging tip exerts force on the biological sample being studied. We investigated the sensitivity of neurons and glia to forces exerted by the scanning tip. Neurons were particularly sensitive to tip-applied forces. This is shown in Fig. 3A, where a force of 5 nN damaged neuron N1 part way through the scan and also cut part of the arbor of neuron N2. The neuron N1 was completely removed from the culture dish when scanning force was increased to 10 nN (Fig. 3B). A second example is shown in Fig. 3C,D. After the image shown in Fig. 3C was captured with a force of 5 nN, a force of 60 nN, which reliably removes neurons from the culture substratum (see below) was selectively applied to neuron N2 (boxed area in Fig. 3C,D; image not shown). The increased force removed this neuron from the culture dish as can be seen in Fig. 3D, which is a subsequent image acquired with a scanning force of 5 nN. In separate experiments (data not shown) we have found that it is also possible to perform "nanosurgery" and cut neurites, remove growth cones and even transect single filopodia.

The minimum force which removes neurons from the culture substratum (5-36 nN; $n = 5$) causes no detectable effects on glial cells. Glial cells were removed from the culture substratum only when the imaging force was increased to 60-84 nN ($n = 5$). The differential sensitivity of neurons and glia to tip-applied forces indicates a potential application for AFM, since it may be possible to determine the relative cell adhesion to various substrata by calculating the forces required to peel a cell from the substratum.

The precise mechanism of cell peeling using the AFM is not known. However, our data suggest that when the tip reaches the cell boundary during a horizontal scan, if sufficient vertical force is being applied to the substratum the tip will roll the cell away from the culture substratum. Parpura et al. (unpublished data) have demonstrated at intermediate forces that it is possible to detect this peeling process, since the edge of a cell is rolled, much like a crepe, during the scanning process.

This report demonstrates that it is not only possible to image living cells in three dimensions using AFM, but also

to manipulate them and reveal structural dynamics. The changes in cell morphology observed over time are not restricted to structures on the cell surface. One of the most widely exploited features of the AFM has been its ability to image hard structures at very high resolution (Gould et al., 1990). It is more difficult to image molecules on soft, living cells. However, by using antibodies that have been imaged by AFM (Weisenhorn et al., 1990), it should be possible to locate and visualize specific molecular species on living cells while observing cell surface dynamics. Moreover, taking advantage of the AFM's ability to apply controlled forces to defined cellular locations and to perform nanosurgery, this instrument will make possible the study of cell biology at a level of resolution previously unobtainable with living specimens.

The authors thank T. A. Basarsky, D. Larson, M. McCloskey, A. Myers and D. Sakaguchi for critical reading of this manuscript, and R. Lartius and E. Uemura for help with immunocytochemistry. This work was supported by NSF grants DIR9004649 (E.H.), DIR9113595 (P.G.H.) and NIH grants NS24233 and NS26650 (P.G.H.). P.G.H. is an Alfred P. Sloan Fellow.

REFERENCES

- Binnig, G., Quate, C. F. and Gerber, C. (1986). Atomic force microscope. *Phys. Rev. Lett.* **56**, 930-933.
- Bridgman, P. C. and Dailey, M. E. (1989). The organization of myosin and actin in rapid frozen nerve growth cones. *J. Cell Biol.* **108**, 95-109.
- Bustamante, C., Vesenka, J., Tang, C. L., Rees, W., Guthold, M. and Keller, R. (1992). Circular DNA molecules imaged in air by scanning force microscope. *Biochemistry* **31**, 22-26.
- Gould, S. A. C., Drake, B., Prater, C. B., Weisenhorn, A. L., Manne, S., Hansma, H. G., Hansma, P. K., Massie, J., Longmire, M., Elings, V., Northern, B. D., Mukerjee, B., Peterson, C. M., Stoekenius, W., Albrecht, T. R. and Quate, C. F. (1990). From atoms to integrated circuit chips, blood cells, and bacteria with the atomic force microscope. *J. Vac. Sci. Technol. A* **8**, 369-373.
- Hansma, P. K., Elings, V. B., Marti, O. and Bracker, C. E. (1988). Scanning tunneling microscopy and atomic force microscopy: application to biology and technology. *Science* **242**, 209-216.
- Hansma, H., Vesenka, J., Siefert, C., Kelderman, G., Morret, H., Sinsheimer, R. L., Elings, V., Bustamante, C. and Hansma, P. K. (1992). Reproducible imaging and dissection of plasmid DNA under liquid with the atomic force microscope. *Science* **256**, 1180-1184.
- Hansma, H. G., Weisenhorn, A. L., Edmundson, A. B., Gaub, H. E. and Hansma, P. K. (1991). Atomic force microscopy: seeing molecules of lipid and immunoglobulin. *Clin. Chem* **37**, 1497-1501.
- Henderson, E. (1992). Imaging and nanodissection of individual supercoiled plasmids by atomic force microscopy. *Nucl. Acids Res.* **3**, 445-447.
- Henderson, E., Haydon, P. G. and Sakaguchi, D.S. (1992). Actin filament dynamics in living glial cells imaged by atomic force microscopy. *Science* **257**, 1944-1946.
- Hoh, J. H., Lal, R., John, S. A., Revel, J.-P. and Arnsdorf, M. F. (1991). Atomic force microscopy and dissection of gap junctions. *Science* **253**, 1405-1408.
- Huettnner, J. E. and Baughman, R. W. (1986). Primary culture of identified neurons from the visual cortex of postnatal rats. *J. Neurosci.* **6**, 3044-3060.
- Lartius, R. K. and Uemura, E. (1990). In vitro analysis of astrocyte mediated neurite behavior in the hippocampus of the gray short-tailed opossum. *Soc. Neurosci. Abstr.* **16**, 993.
- Leifer, D., Lipton, S. A., Barnstable, C. J., and Masland, R. H. (1984). Monoclonal antibody to Thy-1 enhances regeneration of processes by rat retinal ganglion cells in culture. *Science* **224**, 303-306.
- Lichtman, J. W., Magrassi, L. and Purves, D. (1987). Visualization of

- neuromuscular junctions over periods of several months in living mice. *J. Neurosci.* **7**, 1215-1222.
- Lindsay, S. M., Nagahara, L. A., Thundat, T., Knipping, U., Rill, R. L., Drake, B., Prater, C. B., Weisenhorn, A. L., Gould, S. A. C. and Hansma, P. K.** (1989). STM and AFM images of nucleosome DNA under water. *J. Biomol. Struct. Dynam.* **7**, 279-287.
- Mattson, M. P. and Kater, S. B.** (1989). Development and selective neurodegeneration in cell cultures from different hippocampal regions. *Brain Res.* **490**, 110-125.
- Tomie, T., Shimizu, H., Majima, T., Yamada, M., Kanayama, T., Kondo, H., Yano, M. and Ono, M.** (1991). Three-dimensional readout of flash X-ray images of living sperm in water by atomic force microscopy. *Science* **252**, 691-693.
- Weisenhorn, A. L., Egger, M., Ohnesorge, F., Gould, S. A. C., Heyn, S.-P., Hansma, H. G., Sinsheimer, R. L., Gaub, H. E. and Hansma, P. K.** (1991). Molecular-resolution images of Langmuir-Blodgett films and DNA by atomic force microscopy. *Langmuir* **7**, 8-12.
- Weisenhorn, A. L., Gaub, H. E., Hansma, H. G., Sinsheimer, R. L., Kelderman, G. L., and Hansma, P. K.** (1990). Imaging single-stranded DNA, antigen-antibody reaction and polymerized Langmuir-Blodgett films with an atomic force microscope. *Scanning Microsc.* **4**, 511-516.

(Received 10 August 1992 - Accepted 13 October 1992)